Redox Biology 15 (2018) 548–556

Contents lists available at ScienceDirect

Redox Biology

journal homepage: www.elsevier.com/locate/redox

Research Paper

Lipophilic ester and amide derivatives of rosmarinic acid protect cells against H_2O_2-induced DNA damage and apoptosis: The potential role of intracellular accumulation and labile iron chelation

Paraskevi S. Gerogianni[a], Maria V. Chatziathanasiadou[b], Dimitrios A. Diamantis[b], Andreas G. Tzakos[b], Dimitrios Galaris[a,*]

[a] Laboratory of Biological Chemistry, School of Health Sciences, Faculty of Medicine, University of Ioannina, 45110 Ioannina, Greece
[b] Laboratory of Organic Chemistry and Biochemistry, School of Natural Sciences, Department of Chemistry, University of Ioannina, 45110 Ioannina, Greece

ARTICLE INFO

Keywords:
Cell apoptosis
DNA damage
Labile iron
Oxidative stress
Rosmarinic acid derivatives
Cell uptake

ABSTRACT

Phenolic acids represent abundant components contained in human diet. However, the negative charge in their carboxylic group limits their capacity to diffuse through biological membranes, thus hindering their access to cell interior. In order to promote the diffusion of rosmarinic acid through biological membranes, we synthesized several lipophilic ester- and amide-derivatives of this compound and evaluated their capacity to prevent H_2O_2-induced DNA damage and apoptosis in cultured human cells. Esterification of the carboxylic moiety with lipophilic groups strongly enhanced the capacity of rosmarinic acid to protect cells. On the other hand, the amide-derivatives were somewhat less effective but exerted less cytotoxicity at high concentrations. Cell uptake experiments, using ultra-high performance liquid chromatography coupled with tandem mass spectrometry (UHPLC-MS/MS), illustrated different levels of intracellular accumulation among the ester- and amide-derivatives, with the first being more effectively accumulated, probably due to their extensive hydrolysis inside the cells. In conclusion, these results highlight the hitherto unrecognized fundamental importance of derivatization of diet-derived phenolic acids to unveil their biological potential.

1. Introduction

It has been established that the rate of monovalent reduction of O_2 is increased inside the cells under a variety of conditions, leading to elevated steady state concentration of reactive oxygen species (ROS), the most important of which is H_2O_2. Thus, complex mechanisms have been evolved to sense changes of intracellular H_2O_2 and cells respond according to the intensity and duration of stress [1]. We have recently shown that the intracellular labile iron level represents a key determinant to cell response in conditions of oxidative stress by regulating redox signaling through MAP kinases [2,3]. Interestingly, a plethora of natural products can penetrate through biological membranes and by modulating intracellular labile iron level to determine cell fate in conditions of elevated oxidative stress [3–5]. Based on these observations, our scientific interest has focused on evaluating the capacity of iron-chelating natural products, contained in human diet, to penetrate through biological membranes and act inside the cells.

Humans take up daily large amounts of natural phenolics, which are contained in plant-derived foods. It has been proposed that the consumption of phenolic compounds contributes to the maintenance of human health by exerting anti-tumor, anti-inflammatory, anti-viral and antioxidant properties [6–12]. However, the real biochemical basis for these effects remains poorly understood and the accumulated experimental data are highly controversial [6,13–15]. The prevailing hypothesis suggests that phenolic compounds act mainly as “antioxidants” or “free radical scavengers”. However, this proposal lacks direct experimental support, as large prospective studies using classical antioxidant compounds were negative [16–20].

Rosmarinic acid (RosA, O-caffeoyl-3,4-dihydroxyphenyl lactic acid) is a naturally occurring polyphenolic compound, which is abundantly distributed in herbs, such as rosemary, sweet basil and perilla [21]. It possesses two ortho-dihydroxyl (catecholic) groups and one carboxylic group in its core. It has to be stressed, however, that the presence of the negative charge in the carboxylic group limits the capacity of RosA to penetrate through cell membranes and strongly prevents its intracellular action. Despite this limitation, RosA has been reported to

Abbreviations: ACN, acetonitrile; DTT, dithiothreitol; FBS, fetal bovine serum; FITC, fluorescein isothiocyanate; G.O., glucose oxidase; JNK, c-Jun NH2-terminal kinase; MAPKs, mitogen activated protein kinases; PI, propidium iodide; ROS, reactive oxygen species; RosA, rosmarinic acid; SIH, salicylaldehyde isonicotinoyl hydrazine

* Correspondence to: Laboratory of Biological Chemistry, University of Ioannina, School of Health Sciences, Department of Medicine, 451 10 Ioannina, Greece.
E-mail address: dgalaris@uoi.gr (D. Galaris).

https://doi.org/10.1016/j.redox.2018.01.014
Received 12 January 2018; Received in revised form 24 January 2018; Accepted 31 January 2018
Available online 02 February 2018

influence the activities of intracellular enzymes, such as lipoxygenases, cycloxygenases and prolyl hydroxylases [22–25] and transcriptional factors, such as NF-kB and STAT3 [26–28], all of which are involved in the process of inflammation.

Interestingly, there are many cases where ester derivatives of phenolic acids appeared to be more effective than their parent compounds [5,7–10,28,29]. We hypothesized that chemical capping of the negative charge of the caboxilic group in RosA through ester- or amide-derivatives should improve its bioactivity profile by enhancing its cell permeability potential. Thus, the aim of the present study was to explore the influence of esterification or amidation of the carboxylic group of RosA on its ability to protect cultured cells against H_2O_2-induced DNA damage and apoptosis and to examine the potential underlining mechanisms.

2. Materials and methods

2.1. Materials

RPMI-1640 growth medium supplemented with L-glutamine and glucose oxidase (from Aspergillus niger, 18,000 units/g) were obtained from Sigma-Aldrich (St. Louis, MO, USA). Fetal bovine calf serum (FBS), Nunc tissue culture plastics, low melting-point agarose and penicillin/streptomycin antibiotics were obtained from Gibco GRL (Grand Island, NY, USA). Microscope superfrosted glass-slides were supplied by Menzel-Glaset (Menzel, Germany). Calcein-AM was from Molecular Probes (Eugene, OR, USA). Formic acid (LC-MS grade, 98%) was obtained from Fluka. Regenerated cellulose membrane filters with 0.2 μm pore size and 4 mm diameter were purchased from Phenomenex. A Kinetex C18 column 100 mm × 2.1 mm, 2.6 μm column was purchased from Phenomenex, USA. The specific iron chelator SIH (salicylaldehyde isonicotinoyl hydrazone) was a kind donation from Professor Prem Ponka (McGill University, Montreal, QC, Canada). All other chemicals used were of analytical grade.

2.2. Cell cultures

Jurkat cells (ATCC, clone E6-1) were grown in RPMI-1640 containing 10% heat-inactivated FBS, 2 mM glutamine, 100 U/ml penicillin and 100 ng/ml streptomycin, at 37 °C in 95% air and 5% CO_2. Jurkat cells in the log phase were harvested by centrifugation (250 *g*, 10 min), resuspended at a density of 1.5×10^6 cells per ml and allowed to stay for 1 h under standard culturing conditions before treatments.

2.3. Measurement of H_2O_2 generation

The amount of H_2O_2 generated by the enzyme "glucose oxidase" (G.O.) in PBS containing 5.0 mM glucose (in the absence of cells) was estimated either by measuring the increased absorbance at 240 nm (molar absorption coefficient 43.6 M^{-1} cm^{-1}) or by polarographic detection of liberated O_2 with an oxygen electrode (Hansatech Instruments, King's Lynn, Norfolk, UK). The accumulated H_2O_2 was estimated by addition of excess catalase. Addition of RosA to the reaction mixture at concentrations comparable to those used in the experiments did not affect the rate of H_2O_2 production by glucose oxidase (data not shown).

2.4. Synthesis of RosA-ester and -amide derivatives

The chemical synthesis of RosA-ester (RosA-propyl ester and RosA-phenethyl ester) and RosA-amide (RosA-propyl amide and RosA-phenethyl amide) derivatives was made according to the steps illustrated in Fig. 1**A**. Detailed description of the synthetic methodology as well as the characterization of the compounds is presented as "Supplementary material".

2.5. Evaluation of the protection offered against H_2O_2-induced DNA damage

Cells were treated with each compound for the time periods indicated under otherwise standard culture conditions, and then exposed for 10 min to continuously generated H_2O_2 formed by the action of the enzyme "glucose oxidase" which was added directly to growth medium. The amount of the enzyme added was estimated to generate approximately 10 μM of H_2O_2 per min. Cells were then collected and analyzed for formation of single strand breaks in their DNA by comet assay.

The alkaline comet assay was performed essentially as described previously by Singh et al. [30] with minor modifications [31]. In brief, cells were suspended in 1% (w/v) low-melting-point agarose in PBS, pH 7.4, and pipetted onto superfrosted glass microscope slides, precoated with a layer of 1% (w/v) normal melting-point agarose (warmed to 37 °C prior to use). The agarose was allowed to set at 4 °C for 10 min, and the slides were then immersed for 1 h at 4 °C in a lysis solution (2.5 M NaCl, 100 mM EDTA, 10 mM Tris, pH 10, 1% Triton X-100) in order to dissolve cellular proteins and lipids. Slides were placed in single rows in a 30 cm-wide horizontal electrophoresis tank containing 0.3 M NaOH and 1 mM EDTA, pH ~ 13 (unwinding solution) and kept at 4 °C for 40 min in order to allow DNA strand separation (alkaline unwinding). Electrophoresis was performed for 30 min in the unwinding solution at 30 V (1 V/cm) and 300 mA. Finally, the slides were washed for 3 × 5 min in 0.4 M Tris (pH 7.5, 4 °C) and stained with Hoechst 33342 (10 mg/ml).

Hoechst-stained nucleoids were examined under a UV-microscope with a 490 nm excitation filter at a magnification of ×400. DNA damage was not homogeneous, and visual scoring was based on the characterization of 100 randomly selected nucleoids, as previously described [31]. In brief, the comet-like DNA formations were categorized into five classes (0, 1, 2, 3 and 4) representing an increasing extent of DNA damage visualized as a 'tail'. Each comet was assigned a value according to its class. Accordingly, the overall score for 100 comets ranged from 0 (100% of comets in class 0) to 400 (100% of comets in class 4). In this way the overall DNA damage of the cell population can be expressed in arbitrary units.

2.6. Evaluation of cell uptake by using UHPLC-MS/MS

Jurkat cells (3×10^6 cells per well) were seeded into six-well plates and treated with 50 μM of each compound for the time periods indicated under otherwise standard culture conditions. At the indicated time points (5, 10, 20, 30 and 60 min), cells were collected, rinsed twice with PBS and lysed in an ice-cold solution of acetonitrile (ACN):dH_2O (3:1 v/v). Then the samples were centrifuged and the liquid phase of supernatants was evaporated to dryness using speedvac SPD1010 (Thermoscientific, USA). Finally, the samples were reconstituted at ACN:dH_2O (25%:75% v/v) solution and 2 μl of each sample were injected automatically by a PAL autosampler system (CTC Analytics AG, Switzerland) for LC-MS/MS analysis. To estimate the peak area at 100% cell uptake, analytes (50 μM) were added in lysed cells.

Liquid chromatography was performed using a Bruker Advance UHPLC system (Bruker, Germany). A Kinetex C18 column 100 mm × 2.1 mm, 2.6 μm column (Phenomenex, USA) was used as stationary phase and set to 40 °C. The mobile phase was composed of deionized water and ACN, both containing 0.1% formic acid. The following gradient profile, at a constant flow rate of 250 μl/min, was used: the initial phase concentration 5%, increased to 100% within 2 min, then kept constant for 2 min and reduced to 5% till the end of the run. The analysis run time was 5 min and the RT of RosA, RosA-propyl amide, RosA-phenethyl amide, RosA-propyl ester, RosA-phenethyl ester were 2.3, 2.38, 2.51, 2.58 and 2.69 min, respectively. The EVOQ Elite ER triple quadrupole mass spectrometer (Bruker Daltonics, Germany) was utilized for the detection of the five analytes. The mass spectrometer was operated on negative ionization electrospray mode (ESI-). The

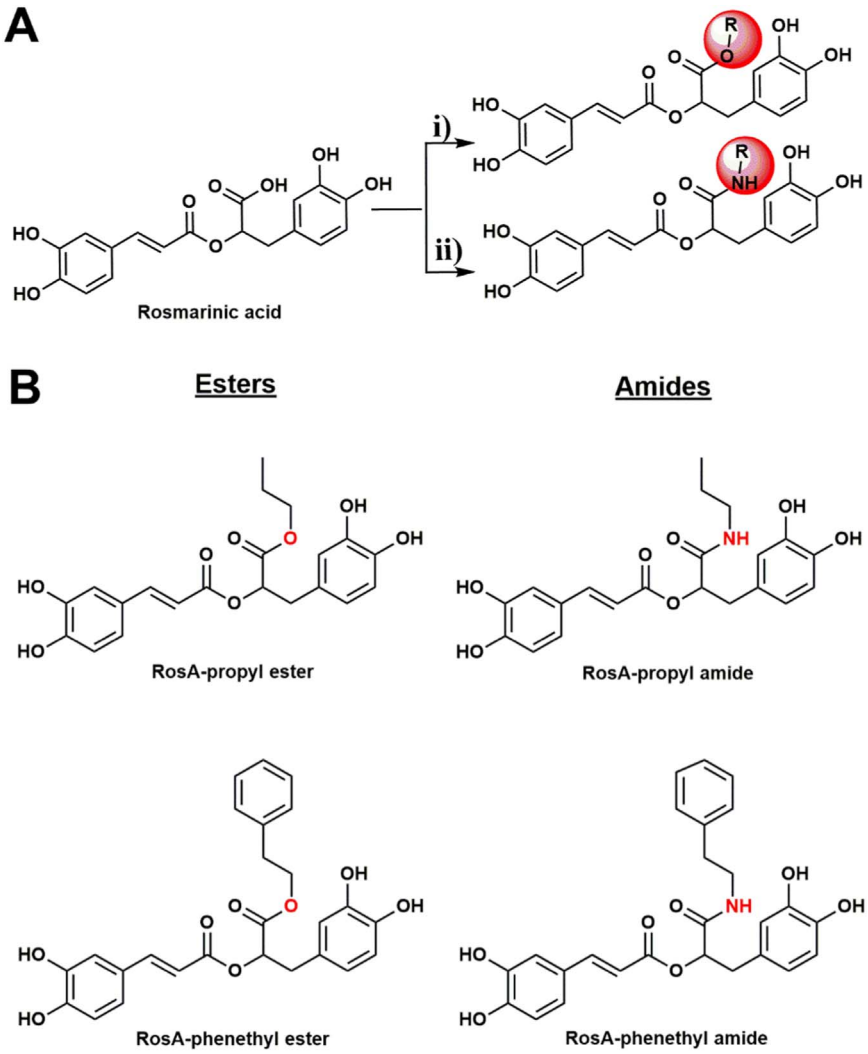

Fig. 1. (A) General scheme depicting the chemical synthesis of RosA-ester (i) and RosA-amide (ii) derivatives used in this work. (B) The chemical structures of synthesized compounds.

spray voltage (−) was set to 5000 V, the heated probe gas flow to 50 units, the heated probe temperature at 300 °C, the cone gas flow to 20 units, the cone temperature at 350 °C and the nebulizer gas flow to 50 units. Using MRM builder, a tool for multiple reaction monitoring (MRM), the optimal MRM transitions were selected for the quantitation of the analytes: RosA (*m/z* 359→161), RosA-propyl ester (*m/z* 401→179), RosA-propyl amide (*m/z* 400→178.9), RosA-phenethyl ester (*m/z* 463.1→179) and RosA-phenethyl amide (*m/z* 462→179). Total data were collected and processed using the MSWS 8.2 software provided by Bruker.

2.7. Evaluation of H_2O_2-induced apoptosis

Jurkat cells were seeded into six-well plates at a density of 3×10^6 cells per well (1.5×10^6 cells/ml) and left for 1 h in the incubation chamber. The cells were then treated with the tested compounds at the indicated concentrations for 30 min and exposed to a bolus addition of 250 μM H_2O_2. After 7 h the cells were collected, centrifuged and cell pellets were suspended in calcium buffer 1× (10 mM Hepes, pH = 7.4, 140 mM NaCl, 2.5 mM $CaCl_2$) at a rate of 10^5 cells/100 μl. Cells were stained with 5 μl of Annexin V-Fluorescein isothiocynate (FITC) and 5 μl of 50 μg/ml of propidium iodide (PI). Each sample was incubated for 30 min in the dark at room temperature. FITC and PI fluorescence were then determined in a flow cytometer apparatus (Partec ML, Partec GmbH, Germany).

2.8. Estimation of intracellular labile iron

Intracellular labile iron was assayed basically as described before by Epsztejn et al. [32], with minor modifications [33,34]. Briefly, after the indicated treatments, cells were washed and incubated with 0.15 μM calcein-AM for 15 min at 37 °C in PBS containing 1 mg/ml BSA and 20 mM Hepes, pH 7.3. After calcein loading, cells were washed, re-suspended in 2.2 ml of the same buffer without calcein-AM, placed under stirring in a fluorescence spectrophotometer (F-2500; Hitachi) cuvette and fluorescence was monitored (excitation 488 nm; emission 517 nm). Calcein-loaded cells show a fluorescence component (ΔF) that is quenched after binding of intracellular iron. Thus, the quenching was minimized by the addition of 11 μM SIH, a highly specific and membrane-permeant iron chelator, and the increase in fluorescence was analogous to calcein chelated iron. Cell viability (assayed as Trypan Blue exclusion) was > 95%, and was unchanged during the assay.

2.9. Preparation of protein extracts

Total cellular protein extracts were prepared by lysing 3×10^6 cells (1.5×10^6 cells/ml) in lysis buffer (50 mM Tris-HCl, pH = 7.5, 150 mM NaCl, 1% Triton X-100, 0.5% sodium deoxycholate, 0.1% SDS), 1× cocktail inhibitors of proteases and phosphate inhibitors (2 mM sodium orthovanadate, 20 mM β-glycerol phosphate and 10 mM NaF). The mixture was incubated for 30 min on ice and centrifuged at 14.000 × *g* for 30 min at 4 °C. Protein concentrations in supernatants

were determined by the Bradford method, using bovine serum albumin as a standard. The samples were then stored until final analysis.

2.10. Western blotting

For immunoblotting analysis, 30–50 μg of protein were loaded with Laemmli Buffer, boiled with DTT, separated by SDS-polyacrylamide gel electrophoresis, and transferred to nitrocellulose membranes by electroblotting. After blocking with 5% non-fat milk, membranes were incubated with specific antibodies against ferritin heavy chain, followed by horseradish peroxidase-conjugated secondary antibodies. Band quantifications were performed by QuantityOne (Bio-Rad Laboratories).

2.11. Statistical analysis

Results were expressed as the mean ± SEM. Significant differences ($P \leq 0.05$) were determined by one-way analysis of variance (ANOVA) followed by Tukey's post hoc test for multiple comparisons between groups. Relationship between two variables was assessed by Spearman's rank correlation coefficient.

3. Results

Propyl- and phenethyl-ester and -amide derivatives of RosA were synthesized, as described in Materials and Methods (Fig. 1**A**). The chemical structures of the synthesized compounds which were tested in this work are illustrated in Fig. 1**B**.

The degree of DNA protection offered by each derivative, when added to cells 20 min before the exposure to H_2O_2, was evaluated in Jurkat cells by using the comet assay methodology, as previously reported for other phenolic compounds [4,5]. As shown in Fig. 2, pre-incubation of the cells with RosA offered a slight protection at high concentrations ($IC_{50} > 500$ μM). Based on our previous findings that compounds bearing the ortho-dihydroxyl moiety were able to chelate labile iron and thereby to prevent H_2O_2-induced DNA damage [4,5], we hypothesized that the low effectiveness of RosA emanated from its inability to penetrate through plasma membrane due to negatively charged carboxylic group. Indeed, esterification of RosA increased dramatically the protective capacity of RosA, as shown in Fig. 2**A** and **B**. The IC_{50}s were estimated ~ 25 and ~ 12 μM for propyl ester and phenethyl ester, respectively. However, it was also observed that the protection offered by RosA-phenethyl ester was lost at the highest concentration used (500 μM). To comprehend the basis for this observation, we tested the effects of the same compounds on DNA integrity in the absence of exogenously added H_2O_2. As shown in Fig. 2**C**, RosA-phenethyl ester was genotoxic at this concentration, inducing DNA single strand breaks in the absence of H_2O_2. The molecular mechanism of RosA-phenethyl ester toxicity is not clear at present.

To evaluate the possibility that the drastic potentiation of RosA effects by its esterification was mediated by hydrolysis of the ester bond catalyzed by cellular non-specific esterases and subsequent accumulation of the generated RosA inside the cells, we synthesized the corresponding RosA amide analogues and tested them in the same experimental system. It was observed that amide derivatives of RosA were much more effective than the parent compound but less effective than the corresponding RosA esters concerning the prevention of H_2O_2-induced DNA damage (IC_{50} = about 75 and 45 μM for RosA-propyl and RosA-phenethyl amide, compared with ~25 and ~12 μM for the corresponding RosA esters) (Fig. 2**A** and **B**). Interestingly, in contrast to RosA-phenethyl ester, the RosA-phenethyl amide was not toxic at the concentration of 500 μM (Fig. 2**B** and **C**). In similar experiments, selective concentrations of the same compounds were tested by using other types of cell lines, like HepG2 liver cells or H1219 lung epithelial cells. Although these cells were generally more resistant than Jurkat cells against H_2O_2-induced damage, the protective effects offered by the

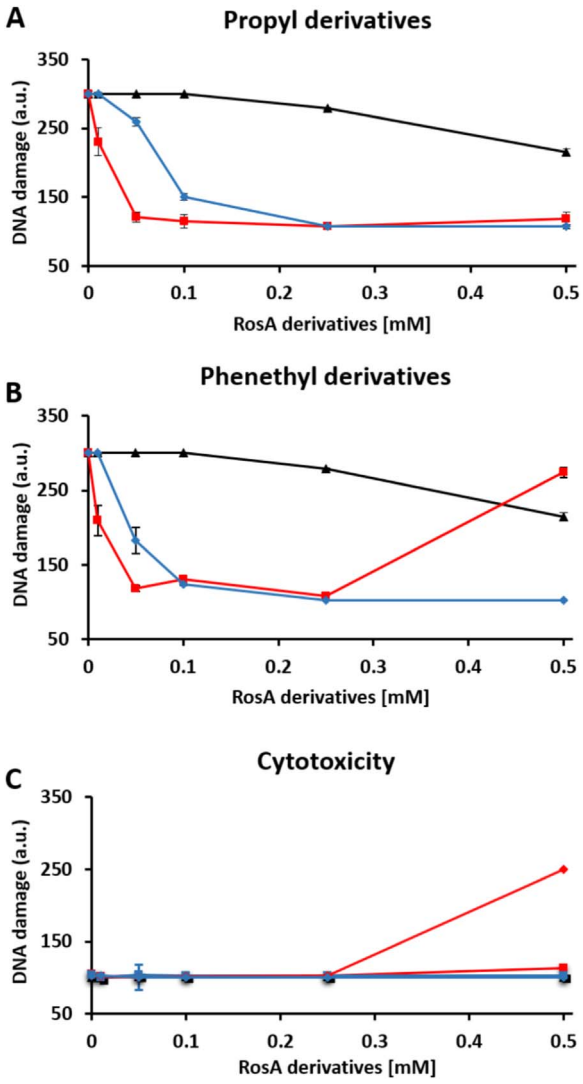

Fig. 2. *Protective effects offered by RosA-ester and RosA-amide derivatives against H_2O_2-induced DNA damage.* Jurkat cells in culture (1.5×10^6 cells/ml) were pre-incubated for 20 min with the indicated concentrations (10, 50, 100, 250 and 500 μM) of RosA (black line) and RosA-propyl ester or RosA-propyl amide (red and blue lines, respectively) (A), or RosA, RosA-phenethyl ester or RA-phenethyl amide (black, red and blue lines, respectively) (B) and then exposed to an amount of glucose oxidase (0.6 μg/ml) able to generate about 10 μM H_2O_2 per minute. After 10 min of exposure to H_2O_2, cells were collected and analyzed for formation of single-strand breaks in their DNA by using the comet assay methodology. (C) Cells were treated with the tested compounds, as in (A) and (B), but were not exposed to H_2O_2. Formation of single-strand breaks in their DNA was measured by using the comet assay methodology. DNA damage was expressed in arbitrary units (a.u.), as described under Materials and Methods. Each point represents the mean ± SD of duplicate measurements in two separate experiments.

tested RA-derivatives were qualitatively similar in all cell types (results not shown).

When the same experiments were performed at low temperature (0–4 °C) instead of 37 °C, the protective capacity offered by RosA ester and amide derivatives remained unchanged, while that of RosA (at concentration 1 mM) was completely lost (Fig. 3). This observation indicates different mechanisms of action for RosA and RosA derivatives. We suggest the latter to be able to diffuse passively through cell membranes, while the parent compound enters the cells through fluid phase endocytosis, in analogy with the known iron chelator desferrioxamin [35].

In order to directly evaluate the rate of cell uptake and the potential accumulation of the tested compounds, we estimated the level of each compound in the treated cells by using UHPLC-MS/MS technology. As

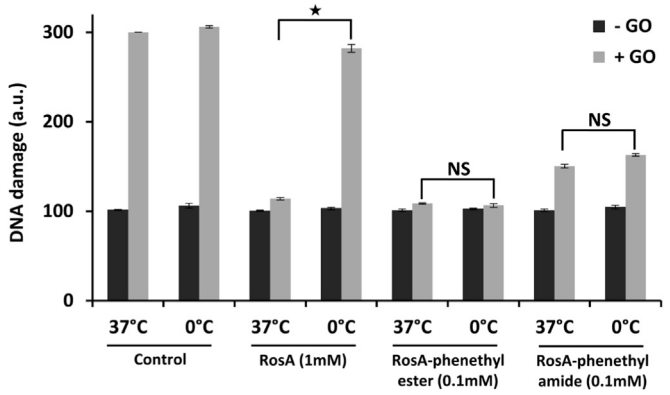

Fig. 3. *Effects of temperature on the capacity of RosA and its phenethyl-ester and phenethyl-amide derivatives to protect cells from H_2O_2-induced DNA damage.* Jurkat cells (1.5×10^6 cells/ml) were pre-incubated for 20 min with vehicle or the tested compounds at 37 °C or at 0 °C before exposure to continuously generated H_2O_2 through the addition of glucose oxidase (G.O.), as in Fig. 2. After 10 min, cells were collected and analyzed for formation of single-strand breaks in their DNA by using the comet assay methodology. Each point represents the mean ± SD of duplicate measurements in two different experiments. The sign * indicates significant difference ($p < 0.05$).

shown in Fig. 4, the parent compound, RosA, was not taken up in significant amounts by the cells at the examined time points. In contrast, the uptake of both ester derivatives was rapid (Fig. 4**A** and **B**), reaching a peak at the first time point measured (5 min). Following, the amount of intracellular propyl ester increased slightly by the time while that of phenethyl ester decreased to about the 50% of the level observed at 5 min. Interestingly, the rate of uptake and the intracellular accumulation were substantially lower for amide derivatives compered to esters, especially at the earliest time point, suggesting differences in uptake and/or accumulation mechanisms.

We next, tested whether RosA-ester and -amide derivatives were able to prevent cell apoptosis, which was initiated by exposure of Jurkat cells to a bolus addition of 250 μM H_2O_2. Seven hours after exposure, cell populations were analyzed by flow cytometry using annexin V and propidium iodide (PI) staining. As shown in Fig. 5, pretreatment of cells with RosA (5, 10, 20 and 50 μM) did not prevent H_2O_2-induced cell apoptosis, while cells pretreated with RosA-phenethyl ester were highly resistant against the same treatment. As in the case of DNA damage, RosA amides were less effective than the corresponding RosA esters, but exerted less cytotoxicity at higher concentrations (Fig. 5**A–C**). The IC_{50}s for the protection offered by the RosA-phenethyl ester and RosA-phenethyl amide were ~ 7.5 and ~ 12 μM, respectively. Similar results were observed when cells were treated with RosA-propyl ester and RosA-propyl amide (Fig. S5A–C), except that the IC_{50}s were ~ 9 and ~ 30 μM for RosA-propyl ester and RosA-propyl amide, respectively and the toxicity of RosA-propyl ester was lower than the corresponding phenethyl ester.

To further elucidate the molecular basis for the protection offered by RosA-ester and -amide derivatives, we used the calcein fluorescence methodology to examine the capacity of the tested compounds to modulate the level of intracellular labile iron. As shown in Fig. 6, treatment of the cells with 100 μM RosA for up to 20 min did not decrease significantly the level of intracellular labile iron pool. In contrast, both RosA-ester and RosA-amide derivatives at the same concentration were effective to reduce significantly the intracellular labile iron (Fig. 6**A** and **B**). In accordance with the DNA protection experiments, RosA-ester derivatives were more effective in reducing intracellular labile iron levels than the corresponding RosA-amide derivatives. As shown in Fig. 6**C**, the protection offered against H_2O_2-induced DNA damage correlated strongly with the capacity of RosA derivatives to decrease intracellular labile iron, indicating that RosA derivatives exert their cytoprotective effect by modulating the levels of intracellular labile iron.

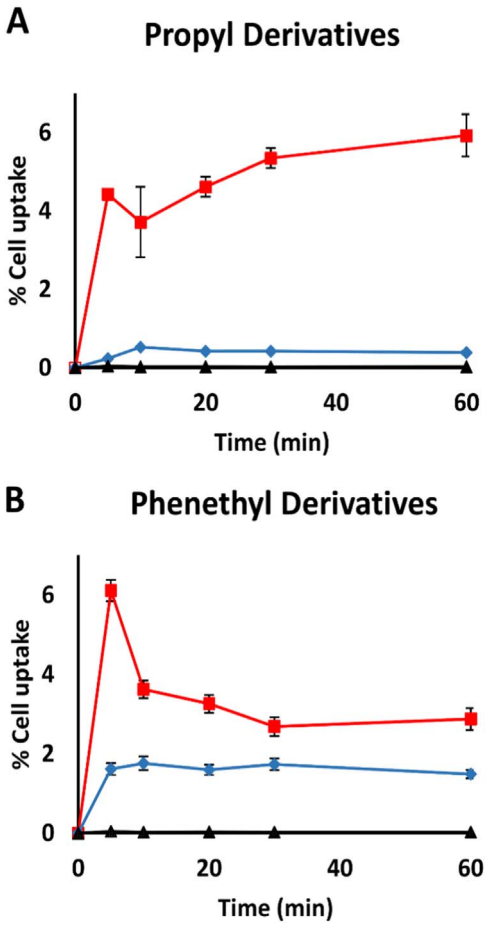

Fig. 4. *Evaluation of cell uptake by using UHPLC-MS/MS.* Jurkat cells were seeded in 6-well plates at a density of 1.5×10^6 cells/ml. The cells were treated with 50 μM of RosA, RosA-propyl ester or RosA-propyl amide (A), and RosA, RosA-phenethyl ester or RA-phenethyl amide (B) for the indicated time periods (5, 10, 20, 30 and 60 min). At the indicated time, cells were collected, rinsed twice with PBS, resuspended in ice-cold solution of ACN:dH_2O (3:1 v/v) for cell lysis and protein precipitation and analyzed for the amount of the tested compounds by using UHPLC-MS/MS as described under Materials and Methods. Black, red and blue lines depict RosA, RosA-ester and RosA-amide derivatives, respectively. The values are expressed as the percentage of the tested amount detected in the cell samples compared to the total amount added in the cell culture medium. Each point represents the mean ± SD of duplicate measurements in two different experiments.

The modulation of intracellular labile iron levels by RosA-ester and -amide derivatives was further substantiated by examining the effects of RosA-phenethyl ester and RosA-phenethyl amide on ferritin heavy chain expression estimated by Western blotting. As shown in Fig. 7, exposure of Jurkat cells to 250 μM H_2O_2 induced a rapid elevation of ferritin heavy chain expression, as previously described [2,3]. Pretreatment of the cells with 20 μM RosA did not exert any significant effect on ferritin increase (Fig. 7**A**), while RosA-phenethyl ester suppressed the ferritin elevation induced by H_2O_2 (Fig. 7**B**). In line with the results described above, RosA-phenethyl amide was less effective in suppressing H_2O_2-induced ferritin elevation compared to RosA-phenethyl ester (Fig. 7**C**).

Taking together, the data presented in this work underline the profound effect exerted by the derivatization of RosA on its capacity to protect cells from damage induced under conditions of oxidative stress. Interestingly, the type of bond (ester or amide) exerted significant influence on both the degree of protection offered and the induced toxicity.

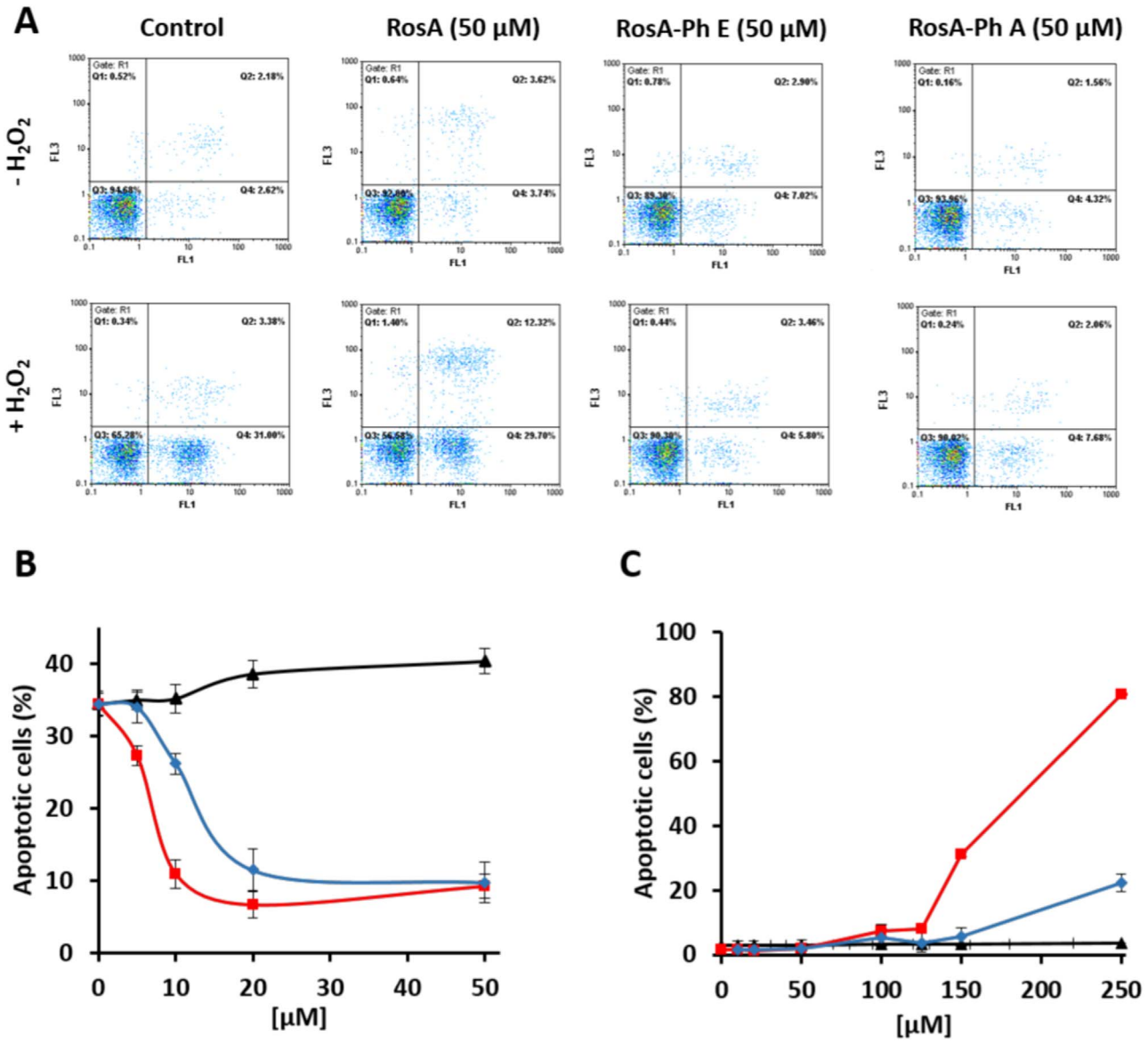

Fig. 5. *Protection against H_2O_2-induced apoptosis offered by RosA-phenethyl ester and RosA-phenethyl amide derivatives.* (A) Jurkat cells (1.5×10^6 cells/ml) were incubated with 50 μM of the indicated compounds for 30 min before the addition of vehicle (upper panels) or 250 μM H_2O_2 (lower panels). Apoptotic cell death was evaluated 7 h later by flow cytometric analysis of Annexin-V binding cells (horizontal axis) and PI staining (vertical axis). (B) The experiments were performed as in (A), except that the indicated concentrations of the tested compounds (5, 10, 20, and 50 μM) were added into the culture medium 30 min before the addition of the H_2O_2. (C) Conditions were as in (A), except that H_2O_2-treatment was omitted. Quantification of apoptotic cells in (B) and (C) was performed by summing the counts of Annexin V-binding cells in Q4 (early apoptotic cells) plus Q2 (late apoptotic cells). Black, red and blue lines depict RosA, RosA-ester and RosA-amide derivatives, respectively. Bars represent the mean percentage of Annexin-V positive cells ± SEM from three independent experiments.

4. Discussion

The main observations of this work were: (i) RosA-ester and -amide derivatives protected cells from H_2O_2-induced DNA damage and cell apoptosis much more effectively than the parent compound. (ii) The protective effects of the synthetic compounds were linked to their increased ability to diffuse through plasma membrane and to chelate labile iron inside cells. (iii) The RosA-ester derivatives were more effective compared to the corresponding RosA-amide ones in the prevention of both H_2O_2-induced DNA damage and cell apoptosis, but the latter exerted less cytotoxicity at higher concentrations. This apparent difference can be explained by the capacity of intracellular non-specific esterases to hydrolyze ester bonds, leading to accumulation of the generated RosA inside the cells, while hydrolysis of the amides, if it takes place at all, must be less effective.

Intracellular labile iron represents the main mediator of peroxide-induced unregulated oxidations in all basic cellular constituents, with serious consequences for many cellular functions [1,36]. Thus, any agent that can modulate intracellular labile iron level also determines the degree of cellular damage in conditions of oxidative stress. Diet, and especially the Mediterranean type of it, contains a plethora of iron chelating components which represent potential modulators of oxidative stress-induced cellular damage. A significant number of plant derived natural compounds contained in diet are phenolic acids or contain a phenolic acid chemotype in their core. Among them, there are many that contain ortho-dihydroxy (catechol) groups in their structure and are able to chelate iron in this group. However, a prerequisite for the protective action of these components is to cross the biological membranes in order to access the cell interior. Most of these acids are unable to influence intracellular peroxide-induced oxidations, because they cannot diffuse through plasma membrane due to the negative charge present in their carboxylic group. Thus, treatment of the cells with high (non-physiological) concentration of RosA was required to observe a slight protection against H_2O_2-induced DNA damage (Fig. 2**A** and **B**).

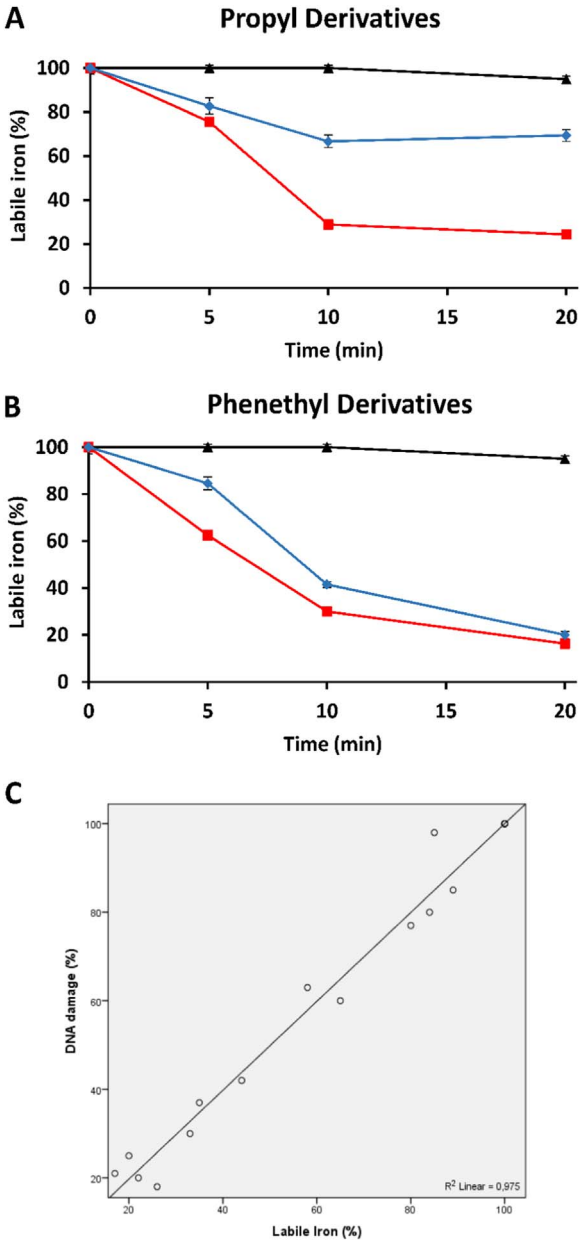

Fig. 6. *Capacity of RosA-ester and RosA-amide derivatives to chelate intracellular labile iron.* The intracellular labile iron level in Jurkat cells was measured by using the calcein method, as described in Materials and Methods. RosA and its propyl (A) and phenethyl (B) ester and amide derivatives at the indicated concentrations were added directly into the cuvette of the fluorometer and the increase in fluorescence was monitored continuously. At the indicated time points (5, 10, 20 min), 11 μM SIH (a membrane-permeable and specific iron chelator) was added and any further fluorescence increase was recorded in order to estimate the percentage of iron still remaining bound to calcein. Black, red and blue lines depict RosA, RosA-ester and RosA-amide derivatives, respectively. The results are presented as the mean ± SEM from three independent experiments. (C) Correlation between the protection offered by RosA derivatives against H_2O_2-induced DNA damage, as estimated by the comet assay, and its ability to decrease intracellular labile iron ($r = 0.975$, $p < 0.001$).

On the other hand, the hydrophobic RosA-ester and RosA-amide derivatives were significantly more effective in protecting cells under the same conditions. Obviously, this effect was based on their increased hydrophobicity, which allows them to diffuse through cell membranes.

Iron was selected during evolution as the main catalyst for biological redox reactions as indicated by its presence in the prosthetic groups of many proteins, either in the form of heme and iron-sulfur clusters or as simple iron atoms. However, when available in redox-active form, it can catalyze reactions that generate extremely reactive free radicals (Fenton-type reactions), able to attack and oxidize all basic cellular constituents [1,37,38]. For this reason, organisms have developed sophisticated molecular mechanisms to tightly regulate iron homeostasis at both cellular and systemic level [39]. Thus, the rapid increase of ferritin expression after exposure of cells to H_2O_2 (Fig. 7) represents a defense response of the cells, since it leads to diminished intracellular labile iron levels. This form of iron is believed to be loosely attached to cellular components at locations which contain oxygen, nitrogen or sulfur. It is obvious, that the positions in which labile iron is attached represent the main targets of the generated reactive free radicals in conditions of oxidative stress. Moreover, any agent that can modulate the intracellular level or the distribution of labile iron influences the points of unregulated oxidation in the case of increased oxidative stress. The emerging new general picture indicates that the catechol group-containing polyphenols of the diet can protect cells and organisms from uncontrolled oxidations by preventing the generation of reactive free radicals close to basic cell constituents. It has to be stressed, that this proposal is in contrast to the prevailing view that antioxidant bioactive compounds scavenge free radicals after their generation.

The observation that RosA derivatives were strong inhibitors of H_2O_2-induced apoptosis (Fig. 5) raises the question about the molecular mechanism(s) involved in this process. We recently reported that intracellular labile iron specifically modulates the prolonged phosphorylation of JNK and p-38 MAP kinases, which determine the decision of cells about survival or death [2,3]. The exact point of iron intervention, however, is still missing and more investigation is needed to elucidate this particular point.

Diffusion and accumulation mechanisms of RosA and its ester- and amide-derivatives in cell are depicted schematically in Fig. 8. Different steps are indicated by numbers: (1) The negative charge in carboxilic group hinders the diffusion of RosA through cell membrane. (2) Lipophilic RosA-ester derivatives diffuse through the plasma membrane and are rapidly hydrolyzed by non-specific esterases inside the cells. The generated RosA is unable to exit the cells due to its charge, and thus, it is trapped and accumulated in the intracellular space. (3) Lipophilic RosA-amide derivatives diffuse through cell membrane, but they are not hydrolyzed (or are hydrolyzed slowly), providing sufficient time available to diffuse out of the cells again.

In conclusion, the results presented in this work highlight the importance of esterification or amidation of phenolic acids for their cell uptake and intracellular actions. It has to be noted, that phenolic acids are often present in nature as esters, combined with a variety of components, while their amide derivatives are less abundant in nature and more difficult to be identified and isolated. Thus, the latter have attracted less attention and have been studied less extensively. Indeed, much still has to be learnt about the role of derivatization of phenolic acids in their uptake, biotransformation, and tissue distribution profile. Moreover, since oxidative stress-induced and labile iron-mediated cell effects are implicated in molecular mechanisms related to serious diseases, specific lipophilic derivatives of phenolic acids may be used for the development of innovative nutraceutical strategies towards the maintenance of human health.

Acknowledgements

This study was partially funded by the General Secretariat for Research and Technology (GSRT) and the Hellenic Foundation for Research and Innovation (HFRI) [grant number 1090].

Conflicts of interest

The authors declare that they have no competing interests.

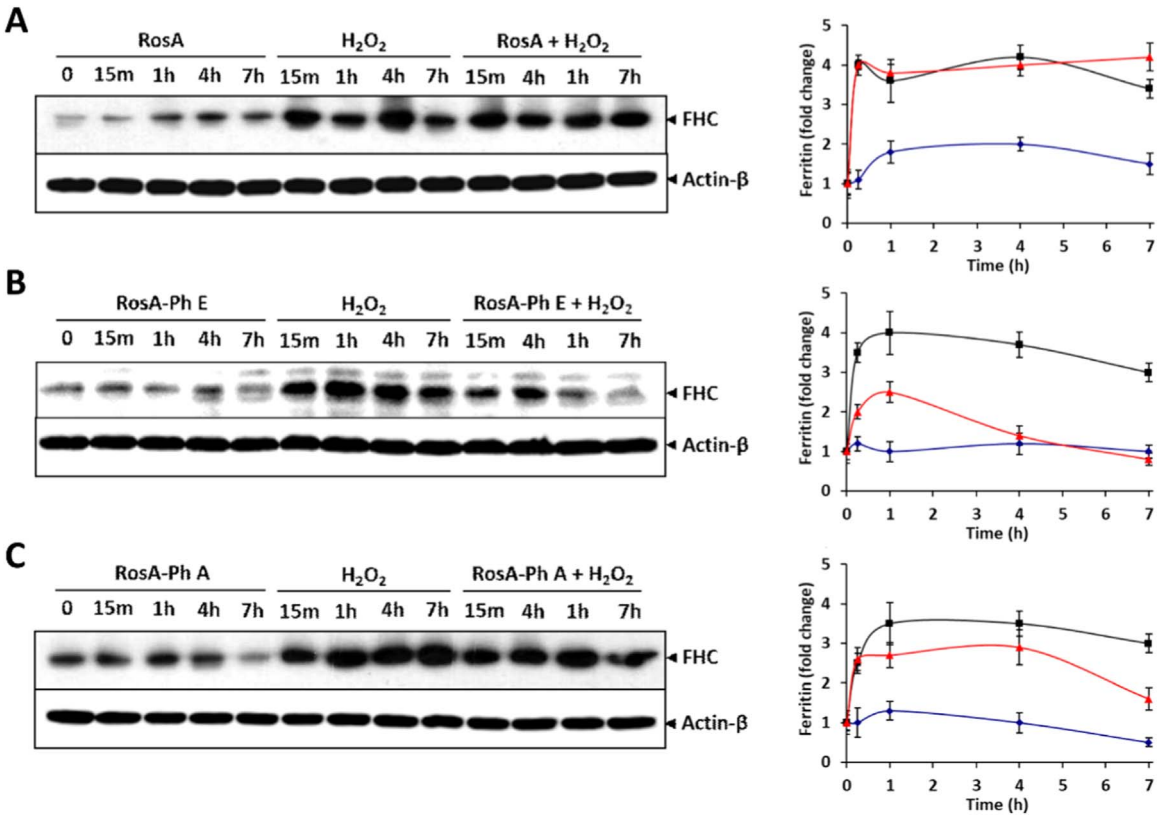

Fig. 7. *RosA-phenethyl ester and RosA-phenethyl amide derivatives mitigate the elevation of ferritin heavy chain (FHC) expression, following exposure of cells to H_2O_2.* Jurkat cells (1.5×10^6 cells/ml) were incubated with 20 μM of the tested compounds RosA, RosA-phenethyl ester and RosA-phenethyl amide (left side on the gel), with 250 μM H_2O_2 alone (middle), or with H_2O_2 plus the tested compound (right side of the gel) for deferent periods. At the indicated time points, cells were collected and total protein lysates were prepared as described in Materials and Methods. The expression of ferritin heavy chain (FHC) was estimated by Western blotting using an antibody that recognized the heavy chain of the protein. Quantification of band intensities is presented in the graphs at right side. Black, red and blue lines depict pretreatment of the cells with RosA, RosA-ester and RosA-amide derivatives, respectively. The results are presented as the mean ± SEM from three independent experiments, expressed as fold change relative to untreated control cells.

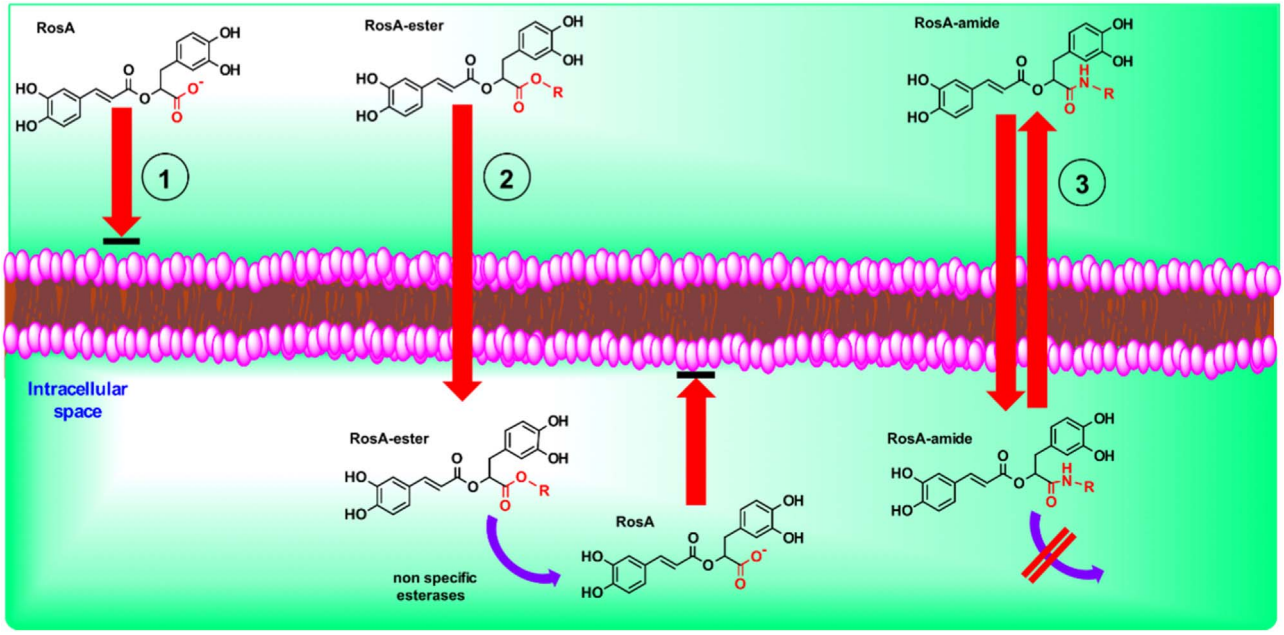

Fig. 8. *Schematic representation of diffusion and accumulation properties of RosA and its ester- and amide-derivatives.* (1) Diffusion of RosA through cell membrane is hindered, due to its negative charge in the carboxilic group. (2) Lipophilic RosA-ester derivatives diffuse easily through the plasma membrane. Inside the cells, they are hydrolyzed by non-specific esterases and the generated RosA is accumulated, because it cannot diffuse out. (3) Lipophilic RosA-amide derivatives diffuse also through cell membrane, but they are not hydrolyzed (or are hydrolyzed slowly). Thus, they have sufficient time available to diffuse out again. Both parent compound and its derivatives are able to chelate intracellular labile iron in their catechol groups when present inside the cells.

Appendix A. Supplementary material

Supplementary data associated with this article can be found in the online version at http://dx.doi.org/10.1016/j.redox.2018.01.014.

References

[1] D. Galaris, K. Pantopoulos, Oxidative stress and iron homeostasis: mechanistic and health aspects, Crit. Rev. Clin. Lab. Sci. 45 (2008) 1–23.

[2] M.D. Mantzaris, S. Bellou, V. Skiada, N. Kitsati, T. Fotsis, D. Galaris, Intracellular labile iron determines H_2O_2-induced apoptotic signaling via sustained activation of ASK1/JNK-p38 axis, Free Radic. Biol. Med. 97 (2016) 454–465.

[3] N. Kitsati, M.D. Mantzaris, D. Galaris, Hydroxytyrosol inhibits hydrogen peroxide-induced apoptotic signaling via labile iron chelation, Redox Biol. 10 (2016) 233–242.

[4] M. Melidou, K. Riganakos, D. Galaris, Protection against nuclear DNA damage offered by flavonoids in cells exposed to hydrogen peroxide: the role of iron chelation, Free Radic. Biol. Med. 39 (2005) 1591–1600.

[5] N. Kitsati, D. Fokas, M.-D. Ouzouni, M.D. Mantzaris, A. Barbouti, D. Galaris, Lipophilic caffeic acid derivatives protect cells against H_2O_2-induced DNA damage by chelating intracellular labile iron, J. Agric. Food Chem. 60 (2012) 7873–7879.

[6] N.R. Prasaud, A. Karthikeyan, S. Karthikeyan, B.V. Reddy, Inhibitory effect of caffeic acid on cancer cell proliferation by oxidative mechanism in human HT-1080 fibrosarcoma cell line, Mol. Cell. Biochem. 349 (2011) 11–19.

[7] H.F. Liao, Y.Y. Chen, J.J. Liu, M.L. Hsu, H.J. Shieh, H.J. Liao, C.J. Shieh, M.S. Shiao, Y.J. Chen, Inhibitory effect of caffeic acid phenethyl ester on angiogenesis, tumor invention, and metastasis, J. Agric. Food Chem. 51 (2003) 7907–7912.

[8] K.-M. Shin, I.-T. Kim, Y.-M. Park, J. Ha, J.-W. Choi, H.-J. Park, U.S. Lee, K.T. Lee, Anti-inflammatory effect of caffeic acid methyl ester and its mode of action through the inhibition of prostaglandin E_2, nitric oxide and tumor necrosis factor-a production, Biochem. Pharmacol. 68 (2004) 2327–2336.

[9] S.K. Kudugunti, N.M. Vad, A.J. Whiteside, B.U. Naik, M.A. Yusuf, K.S. Srivenugopal, M.Y. Moridani, Biochemical mechanism of caffeic acid phenethyl ester (CAPE) selective toxicity towards melanoma cell lines, Chem.-Biol. Interact. 188 (2010) 1–14.

[10] Y.-M. Chiang, C.-P. Lo, Y.-P. Chen, S.-Y. Wang, N.-S. Yang, Y.-H. Kuo, L.-F. Shyur, Ethyl caffeate suppresses NF-kB activation and its downstream inflammatory mediators, iNOS, COX-2, and PGE2 in vitro or in mouse skin, Br. J. Pharmacol. 146 (2005) 352–363.

[11] H. Kikuzaki, M. Hisamoto, K. Hirose, K. Akiyama, H. Taniguchi, Antioxidant properties of ferulic acid and its related compounds, J. Agric. Food Chem. 50 (2002) 2161–2168.

[12] Y.J. Chen, M.S. Shiao, M.L. Hsu, T.H. Tsai, S.Y. Wang, Effect of caffeic acid phenethyl ester, an antioxidant from propolis, on inducing apoptosis in human leukemic HL-60 cells, J. Agric. Food Chem. 49 (2001) 5615–5619.

[13] E.-S. Lee, S.-H. Park, M.S. Kim, S.-Y. Han, H.-S. Kim, Y.-H. Kang, Caffeic acid disturbs monocyte adhesion onto cultured endothelial cells stimulated by adipokine resistin, J. Agric. Food Chem. 60 (2012) 2730–2739.

[14] J.-W. Hwang, E.-K. Kim, S.-J. Lee, Y.-S. Kim, S.-H. Moon, B.-T. Jeon, S.-H. Sung, E.-T. Kim, P.-J. Park, Antioxidant activity and protective effect of anthocyanin oligomers on H_2O_2-triggered G2/M arrest in retinal cells, J. Agric. Food Chem. 60 (2012) 4282–4288.

[15] K. Natarajan, S. Singh, J.R. Burke Jr, D. Grunberger, B.B. Aggarwal, Caffeic acid phenethyl ester is a potent and specific inhibitor of activation of nuclear transcription factor NF-kappaB, Proc. Natl. Acad. Sci. USA 93 (1996) 9090–9095.

[16] A. Warnholtz, T. Munzel, Why do antioxidants fail to provide clinical benefit? Curr. Control Trials Cardiovasc. Med. 1 (2000) 38–40.

[17] S. Hercberg, P. Galan, P. Preziosi, S. Bertrais, L. Memmen, D. Malvy, A.M. Roussel, A. Favier, S. Briancon, The SU.VI.MAX study: a randomized, placebo-controlled trial of the health effects of antioxidant vitamins and minerals, Arch. Intern. Med. 164 (164) (2004) 2335–2342.

[18] I. Bairati, F. Meyer, M. Gelinas, A. Fortin, A. Nabid, F. Brochet, J.P. Mercier, B. Tetu, F. Harel, B. Masse, E. Vigneault, S. Vass, P. del Vecchio, J. Roy, A randomized trial of antioxidant vitamins to prevent second primary cancers in head and neck cancer patients, J. Natl. Cancer Inst. 97 (97) (2005) 481–488.

[19] D. Albanese, O.P. Heinonen, P.R. Taylor, J. Virtamo, B.K. Edwards, M. Rautalahti, A.M. Hartman, J. Palmgren, L.S. Freedman, J. Haapakoski, M.J. Barrett, P. Pietinen, N. Malila, E. Tala, K. Liippo, E.R. Salomaa, J.A. Tangrea, L. Teppo, F.B. Askin, E. Taskinen, Y. Erozan, P. Greenwald, J.K. Huttunen, Alpha-tocopherol and beta-carotene supplements and lung cancer incidence in the alpha-tocopherol, beta-carotene cancer prevention study: effects of base-line characteristics and study compliance, J. Natl. Cancer Inst. 88 (88) (1996) 1560–1570.

[20] C.H. Hennekens, J.E. Buring, J.E. Manson, M. Stampfer, B. Rosner, N.R. Cook, C. Belanger, F. LaMotte, J.M. Gaziano, P.M. Ridker, W. Willett, R. Peto, Lack of long-term supplementation with beta carotene on the incidence of malignant neoplasms and cardiovascular disease, N. Engl. J. Med. 334 (334) (1996) 1145–1149.

[21] M. Petersen, M.S. Simmonds, Rosmarinic acid, Phytochemistry 62 (2003) 121–125.

[22] Y. Kimura, H. Okuda, T. Okuda, T. Hatano, S. Arich, X. Studies on the activities of tannins and related compounds, Effects of coffee tannins and related compounds on arachidonate metabolism in human polymorphonuclear leucocytes, J. Nat. Prod. 50 (1987) 392–399.

[23] D. Choi, J. Han, Y. Lee, J. Choi, S. Han, S. Hong, H. Jeon, Y.M. Kim, Y. Jung, Caffeic acid phenethyl ester is a potent inhibitor of HIF prolyl hydroxylase: structural analysis and pharmacological implication, J. Nutr. Biochem. 21 (2010) 809–817.

[24] S. Yum, H.J. Doh, S. Hong, S. Jeong, D.D. Kim, M. Park, Y. Jung, Piceatannol, a hydroxystilbene natural product, stabilizes HIF-alpha protein by inhibiting HIF prolyl hydroxylase, Eur. J. Pharmacol. 699 (2013) 124–131.

[25] S. Jeong, H. Park, S. Hong, S. Yum, Lipophilic modification enhances anti-colitic properties of rosmarinic acid by potentiating its HIF-prolyl hydroxylases inhibitory activity, Eur. J. Pharmacol. 747 (2015) 114–122.

[26] Y.T. Fan, G.J. Yin, W.Q. Xiao, L. Qiu, G. Yu, Y.L. Hu, M. Xing, D.Q. Wu, X.F. Cang, R. Wang, X.P. Wang, G.Y. Hu, Rosmarinic acid attenuates sodium taurocholate-induced acute pancreatitis in rats by inhibiting nuclear factor-kB activation, Am. J. Chin. Med. 43 (2015) 1117–1135.

[27] H. Ghaffari, M. Venkataramana, B. Ghassam-Jalali, S. Chandra-Nayaka, A. Nataraju, N.P. Geetha, H.S. Prakash, Rosmarinic acid mediated neuroprotective effects against H_2O_2-induced neuronal cell damage in N2A cells, Life Sci. 113 (2014) 7–13.

[28] M. Watabe, K. Hishikawa, A. Takayanagi, N. Shimizu, T. Nakaki, Caffeic acid phenethyl ester induces apoptosis by inhibition of NF-kB and activation of Fas in human breast cancer MCF-7 cells, J. Biol. Chem. 279 (2004) 6017–6026.

[29] P. Wicha, J. Tocharus, A. Nakaew, R. Pantan, A. Suksamran, C. Tocharus, Ethyl rosmarinate relaxes rat aorta by an endothelium-independent pathway, Eur. J. Pharmacol. 766 (2015) 9–15.

[30] N.P. Singh, M.T. McCoy, R.R. Tice, E.L. Schneider, A simple technique for quantitation of low levels of DNA damage in individual cells, Exp. Cell Res. 175 (1988) 184–191.

[31] M. Panagiotidis, O. Tsolas, D. Galaris, Glucose oxidase-produced H_2O_2 induces Ca^{2+}-dependent DNA damage in human peripheral blood lymphocytes, Free Radic. Biol. Med. 26 (1999) 548–556.

[32] S. Epsztejn, O. Kakhlon, H. Glickstein, W. Breuer, I. Cabantchik, Fluorescence analysis of the labile iron pool of mammalian cells, Anal. Biochem. 248 (1997) 31–40.

[33] M. Tenopoulou, P.T. Doulias, A. Barbouti, U. Brunk, D. Galaris, Role of compartmentalized redox-active iron in hydrogen peroxide-induced DNA damage and apoptosis, Biochem. J. 387 (2005) 703–710.

[34] M. Tenopoulou, T. Kurz, P.-T. Doulias, D. Galaris, U.T. Brunk, Does the calcein-AM method assay the total cellular 'labile iron pool' or only a fraction of it? Biochem. J. 403 (2007) 261–266.

[35] P.-T. Doulias, S. Christoforidis, U.T. Brunk, D. Galaris, Endosomal and lysosomal effects of desferrioxamine: protection of HeLa cells from hydrogen peroxide-induced DNA damage and induction of cell-cycle arrest, Free Radic. Biol. Med. 35 (2003) 719–728.

[36] A. Barbouti, P.-T. Doulias, B.-Z. Zhu, B. Frei, D. Galaris, Intracellular iron, but not copper, plays a critical role in hydrogen peroxide-induced DNA damage, Free Radic. Biol. Med. 31 (2001) 490–498.

[37] E.D. Weinberg, The hazards of iron loading, Metallomics 2 (2010) 732–740.

[38] T. Kurz, J.W. Eaton, U.T. Brunk, Redox activity within the lysosomal compartment: implications for aging and apoptosis, Antioxid. Redox Signal. 13 (2010) 511–523.

[39] N. Andrews, Forging a field: the golden age of iron biology, Blood 112 (2008) 219–230.